Control co-design and sensitivity analysis of the LUPA's PTO using WecOptTool

Carlos A. Michelén Ströfer, Michael Devin, Ryan G. Coe, Courtney Beringer, Bret Bosma, Daniel Gaebele, Giorgio Bacelli, and Bryson Robertson

***Abstract*—Control co-design has been shown to significantly improve the performance of wave energy converters (WEC). By considering the control strategy and WEC design concurrently, the space searched by the optimization routine is greatly expanded which results in better performing devices. Recently, we released an open-source WEC co-design code, WecOptTool, to perform control co-design analysis and facilitate its adoption in the community. In this study, we use WecOptTool to perform control co-optimization and uncertainty analysis of the Laboratory Upgrade Point Absorber (LUPA) device. The LUPA can be adjusted to different configurations, including interchanging the drive sprocket. The drive sprocket diameter influences the torque vs speed of the generator, which allows for more flexibility in operating under different wave conditions or with different control schemes. In this study we optimize the drive sprocket diameter, while considering the optimal control algorithm for each potential design, to identify the optimal diameter for electric power production at the PacWave South WEC test site. The power take-off system's (PTO) dynamics are modeled using first principle methods for a parameterized model of the mechanical sub-components in combination with generator model obtained using a power-invariant Park transform. The case-study will be made available to serve as a design tool along the LUPA hardware. Users can readily use this model to perform their own design optimization prior to testing with the physical LUPA device. Finally, we use the automatic differentiation capability of WecOptTool to perform a sensitivity analysis of the power production with respect to the different PTO design parameters.**

***Index Terms*—Control co-design, Sensitivity analysis, Design optimization, Wave energy converters**

I. Introduction

CONTROL co-design has been shown to significantly improve the performance of wave energy converters (WEC) designs [1]–[5]. In this design optimization framework, the controller is optimized simultaneously with all the WEC and power take-off (PTO) parameters of interest. This differs from the sequential approach, which prematurely locks in WEC geometry and power take-off before the control algorithm is optimized. The open source code *WecOptTool*[1] was recently released to allow for easy control co-design of WECs and accelerate the adoption of this design approach in the WEC community.

C. A. Michelén Ströfer, M. Devin, R. G. Coe, D. Gaebele, and G. Bacelli are with Sandia National Laboratories, Albuquerque, NM 87123, U.S.A. (e-mails: [cmichel, mcdevin, rcoe, dgaebele, gbacell]@sandia.gov).

C. Beringer, B. Bosma, and B. Robertson are with Oregon State University, Corvallis, OR 97331, U.S.A. (e-mails: [beringec, bret.bosma, bryson.robertson]@oregonstate.edu).

Digital Object Identifier:
https://doi.org/10.36688/ewtec-2023-288

[1]WecOptTool: https://sandialabs.github.io/WecOptTool

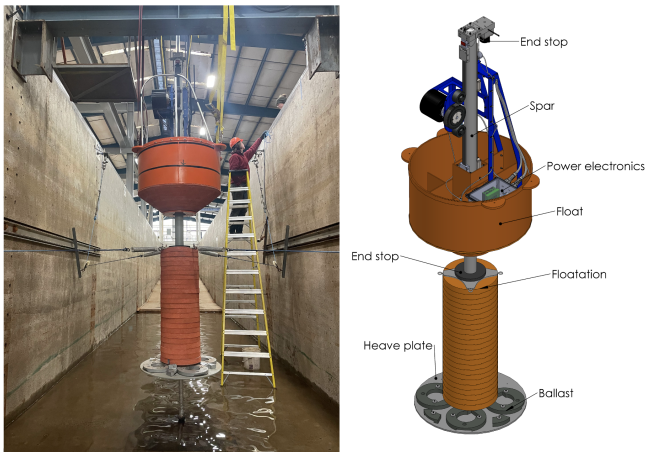

Fig. 1. LUPA WEC: picture (left) with a person for scale, and rendering (right, reproduced with permission from [6]) identifying main components.

This paper presents a co-design and sensitivity study of the Laboratory Upgrade Point Absorber's (LUPA) PTO. LUPA is a laboratory scale WEC developed by Oregon State University as a cost-effective and modular platform for analysing and validating WEC geometry, PTO, and control schemes [6]. The objectives of this study are (i) to demonstrate the use of WecOptTool for design optimization of a real-world application with realistic constraints, (ii) to perform, and demonstrate the approach for, sensitivity analysis and uncertainty quantification using the automatic differentiation capabilities of WecOptTool, and (iii) to provide this case setup to future users of LUPA as a design tool they can use prior to tank testing.

A. LUPA Device

LUPA, shown in Fig. 1, is a scaled open-source WEC designed, fabricated, and tested by Oregon State University [6]. It provides a cost-effective, robust research and development platform for analyzing concepts, validating numerical models, and innovating control schemes in a controlled environment. The base design is a two body point absorber, with the ability to test one or two bodies and to lock-in certain degrees of freedom (e.g. heave-only test). The LUPA also has the ability to exchange different sprockets in the drive-train.

In this study we focus on the LUPA's PTO. For its power transmission system, LUPA uses components manufactured by Gates Corporation. The PTO design

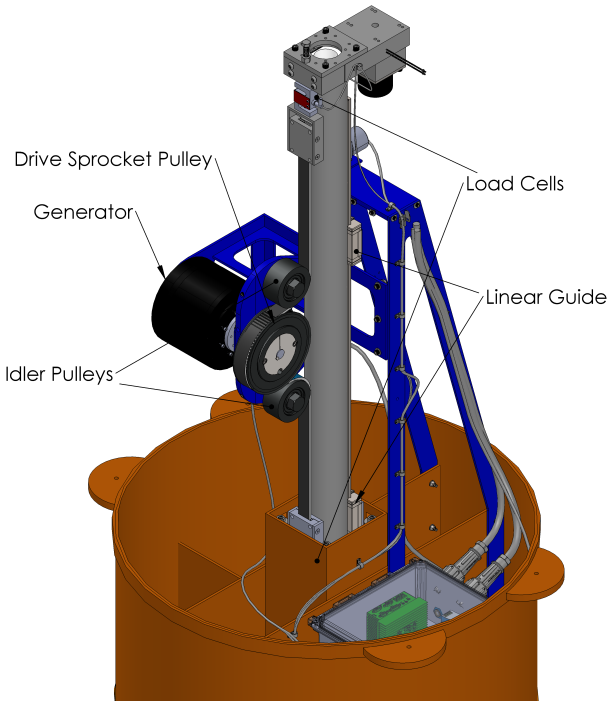

Fig. 2. Rendering of the LUPA's power take-off system with labeled components (reproduced with permission from [6]).

TABLE I
PTO PARAMETERS

Parameter	Symbol	Value
Sprocket diameter	D_s	$0.127\,\mathrm{m}$
Sprocket mom. of inertia	M_s	$0.006\,03\,\mathrm{kg\,m^2}$
Pulley diameter	D_p	$0.108\,\mathrm{m}$
Pulley mom. of inertia	M_p	$0.005\,02\,\mathrm{kg\,m^2}$
Generator mom. of inertia	M_g	$0.017\,86\,\mathrm{kg\,m^2}$
Generator winding resistance	R_g	$5.87\,\Omega$
Generator winding inductance	L_g	$0.0536\,\mathrm{H}$
Generator torque constant	τ_g	$8.51\,\mathrm{N\,m/A}$

is shown in Fig. 2 and consists of a belt-driven system with a sprocket and two idler pulleys. The two idler pulleys are Gates 4.25X2.00-IDL-FLAT, the default sprocket is the Gates 8MX-50S-36, and the generator is model ADR220-B175 by Akribis Systems. The relevant parameters for the PTO model are listed in Table I.

Together with the physical LUPA device, the project specifies different sets of test waves. For each of two locations, four wave conditions are specified for a total of 8 test waves. The two locations are the US DOE PacWave North and PacWave South sites, where a scaling factor of 20 is used for the North site and 25 for PacWave South. The four conditions correspond to the 90$^{\text{th}}$ percentile, the maximum percent annual energy, the maximum occurence, and the 10$^{\text{th}}$ percentile. In this study we use the max occurence wave at PacWave South, which correspond to tank waves with a Pierson—Moskowitz spectra with (1:25 scale) significant wave height of $0.07\,\mathrm{m}$ and peak period $1.90\,\mathrm{s}$.

B. WecOptTool

The WecOptTool is a WEC control co-design tool implemented as two nested optimization loops. The inner loop finds the optimal (structured or unstructured) controller using a pseudo-spectral method [1], [5], [7], [8] while enforcing the dynamic equations and any additional arbitrary constraints in the time domain. The inner loop problem is

$$\begin{aligned} \min_{x} \quad & J(x) \\ & \text{s.t.} \\ & r(x) = 0 \\ & c_{ineq}(x) \geq 0 \\ & c_{eq}(x) = 0, \end{aligned} \tag{1}$$

where x is the state vector which includes the WEC dynamics and controller parameters, $J(x)$ is the objective function (e.g., average electrical power output), $r(x)$ captures the WEC dynamics in residual form, and c_{eq} and c_{ineq} are arbitrary equality and inequality constraints (e.g., maximum line tension or maximum PTO force). The optimal controller can be unstructured, i.e., an arbitrary time-series represented by its Fourier coefficients, or structured, e.g. a PID controller represented by three scalar gains. WecOptTool uses automatic differentiation [9] to solve this inner optimization problem using gradient descent. Gradient descent is the most efficient way to explore the design space, if the function is well behaved and gradients are obtainable, since it uses the gradient information to efficiently find optimal solutions.

In this study we consider the unstructured controller for the PTO force and linear WEC dynamics equations. The linear dynamic equations can be written in the time (t) domain in residual form as

$$\begin{aligned} r(t) &= M\ddot{x} - \sum f(t) \\ &= M\ddot{x} - f_r(t) - f_h(t) - f_f(t) - f_e(t) - f_a(t) \\ &= 0, \end{aligned} \tag{2}$$

where M is a mass/inertia matrix, $\ddot{x}$ the WEC acceleration vector, and the different generalized force vectors are the radiation force f_r due to wave generation, the hydrostatic force f_h, the hydrodynamic frictional force f_f, the wave excitation force f_e, and any additional forces f_a such as PTO force and mooring forces. For a full description of how these terms are modelled, please refer to [1]. The specific additional forces used in this study are described in Section II.

The outer optimization loop considers all other design parameters. These can include WEC geometry parameters as well as PTO parameters. The optimization algorithm is implemented by the user and can be as simple as a brute force or grid optimization. Alternatively, any gradient-free optimization technique can be used.

II. Methodology

The LUPA has several modular components that can be modified, including the number of bodies (1 or 2), the float geometry, the number of degrees of freedom,

the PTO sprocket, and control algorithm. The sprocket diameter affects the speed vs torque of the generator which can have a large effect on the performance of the device under different wave conditions and control algorithms. In this study we perform a PTO control co-design where we find the optimal sprocket diameter while considering the optimal controller for each design. We also look at the sensitivity of LUPA's performance with respect to all the different PTO parameters.

The WEC dynamic equations are the linear WEC dynamic equations described in Section I-B. We consider two additional forces, the PTO force f_p and the mooring force f_m, as

$$f_a = f_p + f_m. \tag{3}$$

The device is modeled in planar motion, with four degrees of freedom: float heave, spar heave, combined surge, and combined pitch. We use the maximum occurrence wave at PacWave South with the 1:25 scale defined by the LUPA project, which corresponds to an irregular wave with Pierson–Moskowitz spectra with significant wave height of $0.07\,\mathrm{m}$ and peak period $1.90\,\mathrm{s}$. We use an unconstrained controller with the PTO force time series (Fourier coefficients) as the control state. The control state is part of inner optimization state, and is therefore arbitrary. The objective function is the average electrical power.

A. PTO model

The objective function is the average electrical power, which means we must model the power conversion chain from PTO force to electricity. The PTO is modeled using 2-port modelling techniques to connect the PTO mechanical and electrical sub-components [10] and a power-invariant Park transform for the generator model (see [1] for more details on the linear PTO model). The linear PTO model can be written based on an impedance that relates the frequency-domain PTO force $\hat{F}_p$ and voltage $\hat{V}$ to the velocity $\hat{U}$ and current $\hat{U}$ as

$$\begin{bmatrix} \hat{F}_p(\omega) \\ \hat{V}(\omega) \end{bmatrix} = Z(\omega) \begin{bmatrix} \hat{U}(\omega) \\ \hat{I}(\omega) \end{bmatrix}. \tag{4}$$

The components of the PTO impedance matrix Z given as

$$Z_{1,1}(\omega) = i\omega \left(\frac{-4}{D_s^2}\right)\left(M_g + M_s + 2\frac{D_s^2}{D_p^2}M_p\right) \tag{5a}$$

$$Z_{1,2}(\omega) = Z_{2,1} = -2\sqrt{6}\frac{\tau_g}{D_s^2} \tag{5b}$$

$$Z_{2,2} = i\omega L_g + B_g. \tag{5c}$$

Here we used the model in [1] with drive-train friction and stiffness both zero, and with drive-train inertia M_d and gear ratio N_d given by

$$M_d = M_g + M_s + 2\frac{D_s^2}{D_p^2}M_p, \tag{6a}$$

$$N_d = \frac{2}{D_s}, \tag{6b}$$

based on the drive-train design (Fig. 2, Table I).

B. Objective function

The impedance matrix can be rearranged into *ABCD* form to give current and voltage as functions of WEC velocity and PTO Force, which we represent in our state vector. The resulting Fourier coefficients represent the time-series of voltage and current, $v(t)$, $i(t)$. We then use the average electrical power as the objective function. The average power is given as the time integral of the product of voltage and current as

$$J(x) = \frac{1}{t_f}\int_0^{t_f} v(t)i(t)\mathrm{d}t \approx \frac{1}{N_t}\sum_{n=0}^{N_t-1} v(t_n)i(t_n). \tag{7}$$

We note that this power is the rate at which the generator is doing work. Electrical power extracted from the system corresponds to a negative average power, which is minimized through (1) to obtain the most power out of the system.

C. Constraints

One of the key features of the pseudo-spectral method in WecOptTool is that you can enforce arbitrary non-linear constraints on the system. The method finds the optimal control strategy to maximize the objective function while respecting the dynamics and constraints. In this study we enforced four realistic constraint based on the LUPA's experimental setup and component specifications. The constraints are as follows:

- **PTO stroke:** The PTO stroke is the relative heave motion of the float and spar and is physically limited to $0.5\,\mathrm{m}$. This limit should be enforced as a soft constraint using the controller, and hence the end-stop dynamics are not directly modeled. Instead, this is specified as a constraint to the pseudo-spectral method (1).
- **Peak generator torque and speed:** The generator manufacturer specifies a maximum torque of $137.9\,\mathrm{N\,m}$ and speed of $15.7\,\mathrm{rad/s}$.
- **Continuous torque:** The generator also has a continuous (RMS) torque rating of $46\,\mathrm{N\,m}$. This is enforced as an upper limit on the root-mean-square (RMS) value of the torque time-series.

D. Mooring

The LUPA setup uses a 4-line taut mooring system with springs connecting the spar to the wall of the wave flume (Fig. 1, left), with a pretension of $285\,\mathrm{N}$ and a line stiffness of $963\,\mathrm{N/m}$. Since seabed interactions are not relevant for this mooring system, the elastic catenary equation can be used to represent the motion of the line, which can be represented in the classic equation given by Irvine [11]:

$$l = \frac{HL_0}{\mathrm{EA}} + \frac{HL_0}{W}[\sinh^{-1}(\frac{V}{H}) - \sinh^{-1}(\frac{V-W}{H})] \tag{8a}$$

$$h = \frac{WL_0}{\mathrm{EA}}\left[\frac{V}{W} - 0.5\right] + \frac{HL_0}{W}\left[\sqrt{1+(\frac{V}{H})^2} - \sqrt{1+(\frac{V-W}{H})^2}\right] \tag{8b}$$

where l and h are the stretched horizontal and vertical lengths of the mooring line, respectively; H and V are the horizontal and vertical tension components of the line at its fairlead, respectively; L_0 is the unstretched line length, W is the wet weight of the line, and EA is the extensional stiffness of the line.

Typically, the differential changes of H and V with respect to l and h can be solved via an iterative numerical solution. However, if we assume the mooring system is symmetric, has no slack in the lines, and the line material and cross sections are linear, the stiffness of the mooring system can be assumed to be at the optimal stiffness $K_I = \mathrm{EA}/L_0$. If we also assume the wet weight of the mooring lines are small compared to the LUPA device, the catenary equation simplifies to an analytical solution given by Al-Solihat and Nahon, which captures nonlinear effects and off-diagonal terms of the mooring stiffness matrix without any significant increase in computational time over the typical linear spring representation of mooring restoring force [12].

The resulting mooring stiffness matrix from [12] abridged to the four planar degrees of freedoms (buoy heave, spar heave, combined surge, and combined pitch) as in this model is given as:

$$K_m = \begin{bmatrix} K_{11} & 0 & 0 & K_{15} \\ 0 & K_{33b} & 0 & 0 \\ 0 & 0 & K_{33s} & 0 \\ K_{51} & 0 & 0 & K_{55} \end{bmatrix} \tag{9}$$

where

$$K_{11} = \frac{1}{2} n \left[\frac{T}{L} (1 + \sin^2 \alpha) + K_I \cos^2 \alpha \right] \tag{10a}$$

$$K_{15} = -n[\frac{T}{2L}(D + D \sin^2 \alpha + R \sin \alpha \cos \alpha) + \frac{K_I}{2}(D \cos^2 \alpha - R \sin \alpha \cos \alpha)] \tag{10b}$$

$$K_{51} = K_{15} \tag{10c}$$

$$K_{33b} = 0 \tag{10d}$$

$$K_{33s} = -n \left[\frac{T}{L} \cos^2 \alpha + K_I \sin^2 \alpha \right] \tag{10e}$$

$$K_{55} = -n\{T \left(D \sin \alpha + \frac{1}{2} R \cos \alpha \right) + \frac{T}{2L}[(R \cos \alpha + D \sin \alpha)^2 + D^2] + \frac{K_I}{2}(D \cos \alpha - R \sin \alpha)^2\} \tag{10f}$$

where D and R are the vertical and horizontal distances from the device center of gravity to the fairlead respectively; n is the number of mooring lines connected, L is the stretched line length, T is the pretension and α is the angle of the mooring lines above the mudline. Refer to [12] for the full derivation of the stiffness matrix.

E. Outer loop

The outer optimization loop considers the different possible sprockets and optimizes for electrical power.

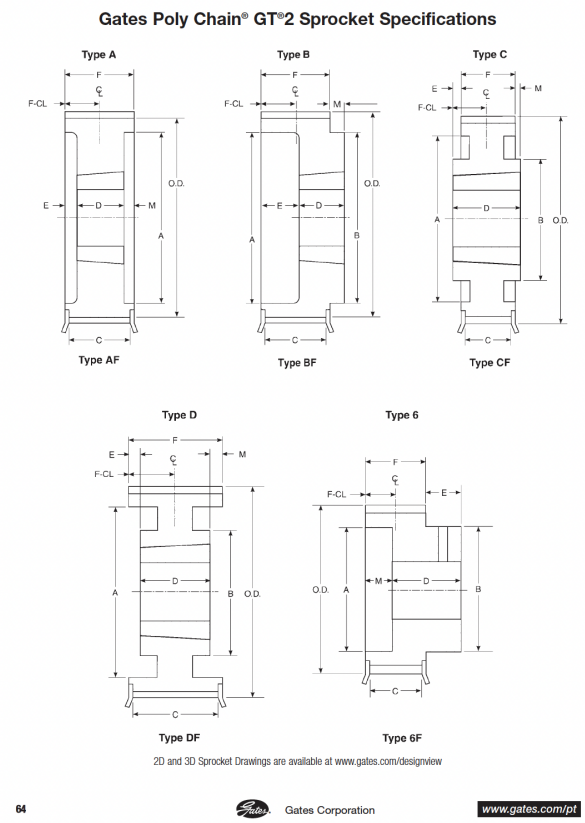

Fig. 3. Manufacturer drawings of the different sprocket shapes. Image reproduced from the 2011 Gates *Drive Design Manual*.

Table II shows the full list of 22 possible Gates sprockets that can be used with LUPA and Fig. 3 shows the different sprocket shapes. The PTO model will use both the sprocket diameter and its moment of inertia, so given the predefined manufacturer designs, these two parameters cannot be considered independently. The sprocket diameter is not the only geometric change between the 22 designs (Fig. 3), making the diameter and moment of inertia have no relationship. However, as will be shown later, the effects of the diameter dominate and an optimal radius can be inferred from the results. The outer optimization loop consists of a brute force sweep through the 22 possible designs (diameter-inertia pairs).

F. Automatic differentiation

Automatic differentiation is a technique for obtaining gradients of code outputs with respect to some input or parameter. Based on the chain rule and the known derivatives of elementary functions, a computational graph can be built for the desired gradient or Jacobian. The Jacobian function has a computational cost in the order of the computational cost of the main function $\mathcal{O}(f)$, and does not scale with number of inputs. This is a huge advantage over numerical gradients which has a cost in the order of $n\mathcal{O}(f)$, i.e. it scales with number of inputs n. Since the pseudo-spectral problem can have hundreds of inputs, WecOptTool was built on top of a differentiable programming framework, `autograd` [9].

One advantage of this is that we are not limited to using the automatic differentiation just for solving the

TABLE II
POSSIBLE SPROCKETS FOR THE LUPA PTO.

Model	Design	Diameter [m]	Mom. of inertia [$\mathrm{kg\,m^2}$]
8MX-32S-36	AF-1	0.0815	0.000843
8MX-33S-36	AF	0.0840	0.000927
8MX-34S-36	AF-1	0.0866	0.00110
8MX-35S-36	AF	0.0891	0.00122
8MX-36S-36	AF-1	0.0917	0.00135
8MX-37S-36	AF	0.0942	0.00164
8MX-38S-36	AF-1	0.0968	0.00169
8MX-39S-36	AF	0.0993	0.00202
8MX-40S-36	AF-1	0.102	0.00206
8MX-41S-36	AF	0.104	0.00240
8MX-42S-36	AF-1	0.107	0.00257
8MX-45S-36	AF-1	0.115	0.00379
8MX-48S-36	AF-1	0.122	0.00480
8MX-50S-36	AF-1	0.127	0.00603
8MX-53S-36	AF-1	0.135	0.00712
8MX-56S-36	AF-1	0.143	0.00931
8MX-60S-36	AF-1	0.153	0.0148
8MX-63S-36	AF-1	0.160	0.0234
8MX-67S-36	DF-1	0.171	0.0129
8MX-71S-36	DF-1	0.181	0.0154
8MX-75S-36	DF-1	0.191	0.0178
8MX-80S-36	BF-1	0.204	0.0507

pseudo-spectral problem (1) but can use it to look at different sensitivities in our design. In this study we look at the sensitivity of the objective function, average electrical power, to the different PTO parameters. The sensitivity of the power P with respect to a parameter Q is $\frac{\partial P}{\partial Q}$ and the normalized sensitivity is $\frac{\partial P}{\partial Q}\frac{Q_0}{P_0}$, where $P_0 = -1.42\,\mathrm{W}$ is the average electrical power of the default design and Q_0 is the default parameter value. The default parameter values are given in Table I.

III. RESULTS

This section presents two different studies. In Section III-A, we use automatic differentiation to look at the sensitivity of the average power at the default design with respect to the eight PTO parameters in Table I. In Section III-B, we solve the full control co-design problem to find the optimal sprocket, out of the 22 options in Table II. This finds the optimal sprocket (outer loop) while considering the optimal controller (inner loop) for each design. An accompanying Jupyter notebook[2] is available to reproduce all these results.

A. Sensitivity analysis for default design

Quantifying the default design's sensitivity to the eight PTO parameters (Table I) requires a function that takes the PTO as input and returns the average electrical power as output. This function first creates the PTO impedance matrix (5) and then solves the

[2]Notebook: https://github.com/cmichelenstrofer/EWTEC_2023

TABLE III
SENSITIVITY OF THE AVERAGE ELECTRICAL POWER TO THE EIGHT PTO PARAMETERS, AT THE DEFAULT DESIGN.

Parameter	Sensitivity		Sensitivity (normalized)
Sprocket diameter	7.90	$\frac{\mathrm{W}}{\mathrm{m}}$	-0.708
Sprocket mom. of inertia	0.170	$\frac{\mathrm{W}}{\mathrm{kg\,m^2}}$	-0.000722
Pulley diameter	-0.0441	$\frac{\mathrm{W}}{\mathrm{m}}$	0.00335
Pulley mom. of inertia	0.473	$\frac{\mathrm{W}}{\mathrm{kg\,m^2}}$	-0.00167
Generator mom. of inertia	0.170	$\frac{\mathrm{W}}{\mathrm{kg\,m^2}}$	-0.00214
Generator winding resistance	0.0864	$\frac{\mathrm{W}}{\Omega}$	-0.357
Generator winding inductance	2.92×10^{-16}	$\frac{\mathrm{W}}{\mathrm{H}}$	-1.10×10^{-17}
Generator torque constant	-0.119	$\frac{\mathrm{W}}{\mathrm{N\,m/A}}$	0.714

objective function (7). All other results are frozen, including the solution to the pseudo-spectral problem (1), i.e., the dynamics and optimal controller time-series. Using the `autograd` package [9] we then create gradient functions and evaluate them at the default design values. The raw and normalized results are presented in Table III.

Since we want power out of the system (negative power) a positive value of the normalized sensitivity indicates a larger value for that parameter is desirable. We are interested in the effect of the sprocket and can see from Table III that a smaller diameter and smaller moment of inertia would result in larger usable power. We can also see that the effect of the moment of inertia is several orders of magnitude smaller than the effect of changing the diameter. Therefore, even though there is no relation between the diameters and moment of inertia of the different sprockets, we can ignore the effect of moment of inertia and draw conclusions on the optimal diameter. This is done in the next section.

The sprocket diameter directly determines the gear ratio (6b) which affects the torque vs. speed of the generator and it was expected to have a very large effect on power, as confirmed by the sensitivity analysis. The results show that a smaller diameter is desirable, which corresponds to a larger gear ratio and the generator operating at faster speeds and lower torque. Lower torque requires less current which translates to less I^2R losses. The results also show that the power is not very sensitive to the drive-train's moment of inertia, but a smaller moment of inertia would be preferable. From (6a) this corresponds to smaller moment of inertia of each component (M_g, M_s, M_p) and larger pulley diameter (D_p), which correspond to the results of the sensitivity analysis.

We can also see that the average power is sensitive to the generator's winding resistance and torque constant, and is not sensitive at all (effectively zero) to the winding inductance. The winding impedance (5c) depends on both the winding resistance B_g and the winding inductance times the frequency ωL_g. The winding inductance L_g is much smaller than the winding resistance

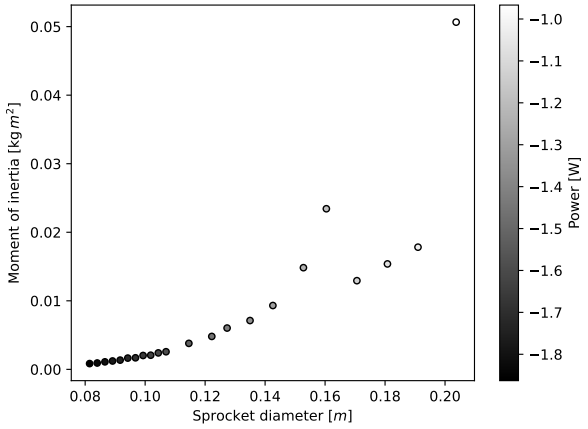

Fig. 4. Results of the sprocket optimization with respect to both sprocket diameter and moment of inertia.

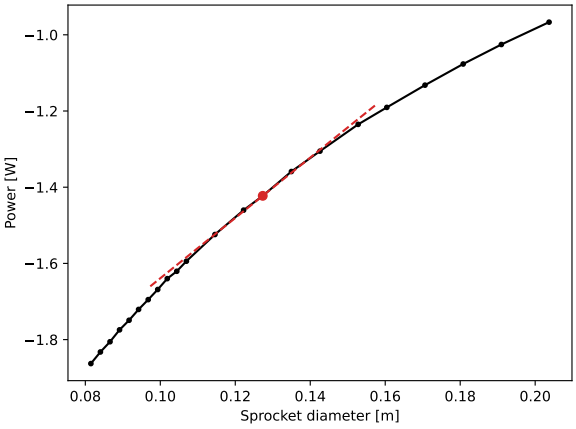

Fig. 5. Results of the sprocket optimization with respect to sprocket diameter.

and the frequencies of ocean waves are small explaining its low sensitivity. The driving electrical losses in the PTO model are the I^2R losses which increase with the winding resistance and current. Current is inversely proportional to the torque constant, explaining why a generator with a larger torque constant and a smaller winding resistance would be expected to produce more power as indicated by the signs of their respective sensibilities in Table III. On a practical note, reducing a generator's winding resistance, or independently increasing it's torque constant are not trivial tasks. A highly efficient generator is usually very costly and the results illustrate that more cost effective improvements can be achieved by ensuring that all components are well coordinated to achieve in phase overall power transfer.

The gradients in Table III can also be used to estimate uncertainty in the physical experiments. As a simple example, if the sprocket diameter can only be measured up to $\Delta D_s = \pm 1\,\mathrm{mm}$ (0.787%), this leads to an uncertainty in the average power of $\frac{\partial P}{\partial D_s}\Delta D_s = \pm 0.0079\,\mathrm{W}$ (0.556%).

B. Sprocket optimization

We are interested in which sprocket, among the list of possible sprockets (Table II) leads to the most power production with the PacWave South maximum occurrence wave. For this we do a brute force optimization looping through each possible sprocket and solving the pseudo-spectral problem for the optimal controller for each. The results are plotted in terms of both diameter and moment of inertia in Fig. 4, and in terms of only diameter in Fig. 5. As expected from the sensitivity analysis, the optimal diameter is smaller than the default, and is actually the lower limit of the range of diameters the LUPA takes. The optimal sprocket is the `8MX-32S-36` with a diameter of $0.0815m$.

Fig. 5 also shows the gradient (red, dashed lines) of power with respect to sprocket diameter at the default design (with sprocket `8MX-50S-36`). This corresponds to the value in Table III of $7.90\frac{W}{m}$. It can be seen that this is in fact the tangent and a very accurate local approximation. This is because although the moment of inertia is also changing, its effect is orders of magnitudes smaller than that of diameter.

IV. Conclusions

The LUPA is a testing platform with many possible configurations and modifications that make it a great tool for researchers. The main PTO component that can be easily swapped is the sprocket. In this study we showed how to use WecOptTool to perform control co-optimization of the sprocket, in order to identify the sprocket that results in the largest average electrical power produced in a specific sea state. Since WecOptTool is built on top of an automatic differentiation platform, we are able to obtain different sensitivities of the design. We used this capability to determine the sensibility of electrical power to each of the eight PTO parameters in the linear PTO model for the LUPA. These sensitivities can be useful not only for informing design modifications, but also for uncertainty quantification. For instance, given some uncertainty in any of the PTO parameters (e.g., based on the measurement technique) this can then be propagated to an uncertainty in the power production. In addition to demonstrating the use of automatic differentiation for sensitivity analysis, we hope this case study serves as a tool that researchers can use to run optimization and sensitivity studies prior to testing the physical LUPA device. To this end we have made this case study available as a Jupyter notebook.

Acknowledgement

This research was supported by the U.S. Department of Energy's Water Power Technologies Office. Sandia National Laboratories is a multi-mission laboratory managed and operated by National Technology and Engineering Solutions of Sandia, LLC., a wholly owned subsidiary of Honeywell International, Inc., for the U.S. Department of Energy's National Nuclear Security Administration under contract DE-NA0003525. This paper describes objective technical results and analysis. Any subjective views or opinions that might be expressed

in the paper do not necessarily represent the views of the U.S. Department of Energy or the United States Government.

REFERENCES

[1] C. A. Michelén Ströfer, D. T. Gaebele, R. G. Coe, and G. Bacelli, "Control co-design of power take-off systems for wave energy converters using wecopttool," *IEEE Transactions on Sustainable Energy*, 2023. [Online]. Available: https://doi.org/10.1109/TSTE.2023.3272868

[2] A. C. O'Sullivan and G. Lightbody, "Co-design of a wave energy converter using constrained predictive control," *Renewable energy*, vol. 102, pp. 142–156, 2017.

[3] P. B. Garcia-Rosa, G. Bacelli, and J. V. Ringwood, "Control-informed optimal array layout for wave farms," *IEEE Transactions on Sustainable Energy*, vol. 6, no. 2, pp. 575–582, 2015.

[4] P. B. Garcia-Rosa and J. V. Ringwood, "On the sensitivity of optimal wave energy device geometry to the energy maximizing control system," *IEEE Transactions on Sustainable Energy*, vol. 7, no. 1, pp. 419–426, 2015.

[5] G. Bacelli, "Optimal control of wave energy converters," PhD, National University of Ireland, Maynooth, Maynooth, Ireland, 2014. [Online]. Available: http://mural.maynoothuniversity.ie/6753/

[6] B. Bosma, C. Beringer, and B. Robertson, "Design and modeling of a laboratory scale wec point absorber," in *Paper presented at the 14th European Wave and Tidal Energy Conference (EWTEC 2021)*, 2021.

[7] G. Bacelli and J. V. Ringwood, "Numerical optimal control of wave energy converters," *IEEE Transactions on Sustainable Energy*, vol. 6, no. 2, pp. 294–302, 2014. [Online]. Available: https://doi.org/10.1109/TSTE.2014.2371536

[8] G. Elnagar, M. Kazemi, and M. Razzaghi, "The pseudospectral Legendre method for discretizing optimal control problems," *IEEE Transactions on Automatic Control*, vol. 40, no. 10, pp. 1793–1796, 1995. [Online]. Available: https://doi.org/10.1109/9.467672

[9] D. Maclaurin, D. Duvenaud, and R. P. Adams, "Autograd: Effortless gradients in numpy," in *ICML 2015 AutoML workshop*, vol. 238, no. 5, 2015.

[10] D. C. Karnopp, D. L. Margolis, and R. C. Rosenberg, *System Dynamics: Modeling, Simulation, and Control of Mechatronic Systems, 5th Edition*. Wiley, 2012. [Online]. Available: https://books.google.com/books?id=8B5guy26PcQC

[11] H. M. Irvine, *Cable Structures*. MIT Press, 1981.

[12] M. K. Al-Solihat and M. Nahon, "Stiffness of slack and taut moorings," *Ships and Offshore Structures*, vol. 11, no. 8, pp. 890–904, 2016. [Online]. Available: https://doi.org/10.1080/17445302.2015.1089052